Chinese Physics B

PAPER

Band engineering of B_2H_2 nanoribbons*

To cite this article: Bao Lei *et al* 2019 *Chinese Phys. B* **28** 046803

Band engineering of B_2H_2 nanoribbons*

Bao Lei(雷宝)[1,2], Yu-Yang Zhang(张余洋)[1,2,3], and Shi-Xuan Du(杜世萱)[1,2,3,†]

[1] *Institute of Physics, Chinese Academy of Sciences (CAS), Beijing* 100190, *China*
[2] *University of Chinese Academy of Sciences, Beijing* 100190, *China*
[3] *CAS Center for Excellence in Topological Quantum Computation, Chinese Academy of Sciences, Beijing* 100190, *China*

(Received 17 January 2019; revised manuscript received 18 February 2019; published online 19 March 2019)

Freestanding honeycomb borophene is unstable due to the electron-deficiency of boron atoms. B_2H_2 monolayer, a typical borophene hydride, has been predicted to be structurally stable and attracts great attention. Here, we investigate the electronic structures of B_2H_2 nanoribbons. Based on first-principles calculations, we have found that all narrow armchair nanoribbons with and without mirror symmetry (ANR-s and ANR-as, respectively) are semiconducting. The energy gap has a relation with the width of the ribbon. When the ribbon is getting wider, the gap disappears. The zigzag ribbons without mirror symmetry (ZNR-as) have the same trend. But the zigzag ribbons with mirror symmetry (ZNR-s) are always metallic. We have also found that the metallic ANR-as and ZNR-s can be switched to semiconducting by applying a tensile strain along the nanoribbon. A gap of 1.10 eV is opened under 16% strain for the 11.0-Å ANR-as. Structural stability under such a large strain has also been confirmed. The flexible band tunability of B_2H_2 nanoribbon increases its possibility of potential applications in nanodevices.

Keywords: borophene hydride nanoribbons, band engineering, first-principles calculations, strain

PACS: 68.35.Gy, 71.15.Mb, 71.20.Ps, 68.60.Wm **DOI:** 10.1088/1674-1056/28/4/046803

1. Introduction

Borophene and its derivatives are important branches in two-dimensional (2D) materials.[1–6] While due to the electron-deficiency of boron, borophene monolayer has been predicted to be structural polymorphism.[7–10] Actually, early synthesized borophene tends to form buckled triangular lattice or planar triangular lattice mixed with different arrangements of hexagonal holes.[11,12] Recently, a planar honeycomb borophene has been synthesized on the Al surface,[13] which was stabilized by compensation charge from the substrate. But the intrinsic properties of honeycomb borophene are deeply affected by the substrate. To get a substrate-free hexagonal borophene, hydrogenation is an alternative strategy to stabilize the honeycomb borophene.[14]

Monolayer B_2H_2, a borophene hydride, consists of honeycomb boron network and bridge hydrogens. It contains three-center-two-electron (3c2e) B–H bonds and is predicted to be a stable structure.[15,16] Recently, B_2H_2 nanosheets are fabricated by exfoliation and complete ion-exchange between protons and Mg cations.[17] Its infinite two-dimensional monolayer sheet has been predicted to exhibit intriguing mechanical properties. B_2H_2 monolayer has also been predicted to undergo a metal-semiconductor transition by applying tensile strain along the zigzag direction with mirror symmetry.[18,19] For integrating into nanoelectronic devices, it is inevitable to manipulate infinite 2D materials into various patterns with finite size, such as nanotubes, nanoribbons, nanodots, and so on. As a reduced-dimensionality form of 2D materials, nanoribbons are extensively investigated.[20–23] Although the B_2H_2 sheets have been investigated, the knowledge about B_2H_2 nanoribbons, which may be used in nanoelectronic devices, is very limited.

In this paper, using quantum mechanical calculations based on density functional theory (DFT), we investigate the electronic structures of B_2H_2 nanoribbons. We have found that the electronic structure of B_2H_2 nanoribbons is sensitive to the ribbon width except for the zigzag ribbon with mirror symmetry (ZNR-s). Narrow ribbons show semiconducting character in general. When the ribbons get wider, a semiconductor-metal transition induced by ribbon width occurs. The possibilities of manipulation to the metallic feature of wide ribbons are further investigated by tensile strain. The armchair nanoribbon without mirror symmetry (ANR-as) and ZNR-s exhibit significant strain effect on band structure. When the strain exceeds a critical level, a band gap is opened. For ANR-as with a width of 11.0 Å, a gap of 1.10 eV is opened under 16% strain. In contrast, for armchair nanoribbon with mirror symmetry (ANR-s) and zigzag ribbon without mirror symmetry (ZNR-as), strain cannot open gap yet. Finally, we also briefly discuss the reasons for the difference in strain effects in 2D infinite B_2H_2 sheet. Above all, the tunability of B_2H_2 nanoribbon electronic

*Project supported by the National Natural Science Foundation of China (Grant Nos. 61888102, 61390501, and 51872284), the CAS Pioneer Hundred Talents Program, the Strategic Priority Research Program of Chinese Academy of Sciences (Grant Nos. XDB30000000 and XDB28000000), the Beijing Nova Program, China (Grant No. Z181100006218023), and the University of Chinese Academy of Sciences.

†Corresponding author. E-mail: sxdu@iphy.ac.cn

properties indicates that it is easier to find application space in nanoelectronic devices.

2. Method

For B_2H_2 nanoribbons, structure optimizations were performed using the plane-wave technique implemented in the Vienna *ab initio* simulation package (VASP).[24] The projected augmented wave method was used to describe the ion-electron interactions, in which the exchange–correlation functional was Perdew–Burke–Ernzerhof (PBE).[25,26] Numerical convergence was achieved with thresholds of 10^{-6} eV in energy and 10^{-2} eV·Å^{-1} in force under a considerable cutoff energy of 400 eV. The *k*-points mesh used in the calculations was $27\times1\times1$ for nanoribbons, generated automatically with the origin at the Γ point. The vacuum layer was larger than 13 Å either in the direction perpendicular to the ribbon plane or the in-plane direction. Different supercell sizes were employed based on various widths of nanoribbons. For example, the supercell size of ANR-as with a ribbon width of 5.1 Å (Fig. 1(a)) is 5.2 Å ×19.0 Å ×16.0 Å, while the size of ZNR-s with a width of 11.3 Å (Fig. 1(d)) is 27.0 Å ×3.0 Å ×16.0 Å. For B_2H_2 monolayer, Γ-point-centered *k*-point of $9\times15\times1$ was applied for the structural relaxation and band structure calculation. The phonon dispersions for B_2H_2 nanoribbons and their 2D counterparts were calculated by density functional perturbation theory (DFPT), which is a well-tested *ab initio* method for accurate phonon calculations.[27] The *q*-mesh for DFPT calculations was sampled with only the Γ point.

3. Results and discussion

The atomic structure of B_2H_2 monolayer is made of in-plane hexagonal boron skeleton and out-of-plane bridged hydrogen pairs. The distance between the two boron atoms bridged by two hydrogen atoms is 1.81 Å, which is longer than the B–B bond length without hydrogen (1.71 Å). The B–H bond distance is 1.33 Å. The electronic property of this B_2H_2 monolayer exhibits metallic character.[15,16,18]

We first explore the band gap dependence on the width of B_2H_2 nanoribbon. For 2D honeycomb material, such as graphene, the commonly researched direction of nanoribbon is along high symmetry direction, that is, armchair and zigzag direction. As for B_2H_2, its high symmetry direction can be classified into two unequal directions, depending on the presence or absence of the mirror symmetry, as shown in Fig. 4(a). In the present work, four investigated types of nanoribbons along high symmetry direction are: armchair nanoribbon without mirror symmetry, armchair nanoribbon with mirror symmetry, zigzag nanoribbon without mirror symmetry, and zigzag nanoribbon with mirror symmetry. The atomic structures are shown in Fig. 1. Due to the saturation with hydrogen atoms at the edges of ribbons, the chemical formula of ribbons varies with the change of ribbon width. For example, the formulas of ANR-as with widths of 5.1 Å and 8.1 Å are B_6H_8 and $B_{10}H_{12}$, respectively, as shown in Fig. 1(a). In addition, the ribbons' formula is also related to the ribbon types. For example, the formulas of ANR-as and ANR-s are B_6H_8 and B_6H_{10}, respectively, with a ribbon width of approximately 5.0 Å, as shown in Figs. 1(a) and 1(b). Here, we have employed unified formula B_2H_2 to describe various nanoribbons for the sake of clarity.

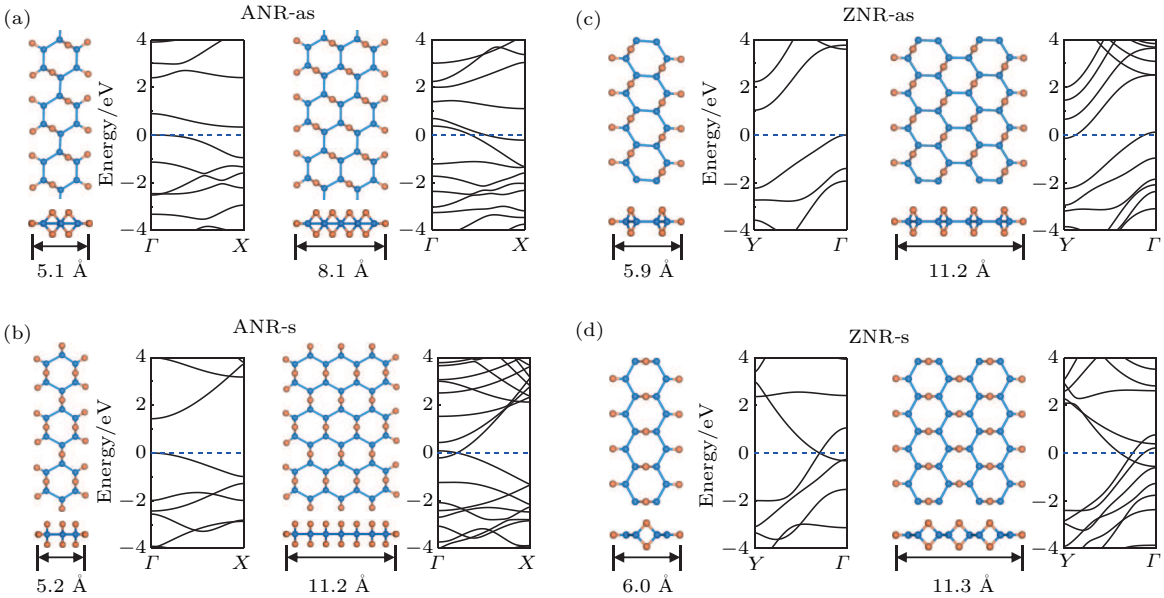

Fig. 1. Atomic structures and band structures of four types of B_2H_2 nanoribbons. Panels (a)–(d) are for ANR-as, ANR-s, ZNR-as, and ZNR-s, respectively. In each panel, atomic structures with different widths and corresponding band structures are presented. Panel (a) is for ANR-as with widths of 5.1 Å and 8.1 Å. Panel (b) is for ANR-s with widths of 5.2 Å and 11.2 Å. Panel (c) is for ZNR-as with widths of 5.9 Å and 11.2 Å. Panel (d) is for ZNR-s with widths of 6.0 Å and 11.3 Å.

An ANR-as with a width of 5.1 Å presents a semiconducting feature with a gap of 0.33 eV. When the width increases, the band gap decreases. Figure 1(a) shows that when the width reaches 8.1 Å, the ANR-as becomes metallic. Comparing to graphene nanoribbon in which there is only one zigzag direction and armchair direction, there are two types of zigzag directions and armchair directions due to the existence of bridged hydrogens. Figure 1(b) shows the atomic structures and electronic structures of ANR-s. For an ANR-s with a width of 5.2 Å, the band gap is 1.44 eV. When the width increases, the gap also decreases. For an 8.2-Å wide ANR-s, the band gap is 0.26 eV. When the width increases to 11.2 Å, the ANR-s becomes metallic, as shown in Fig. 1(b).

The ZNR-as with a width of 5.9 Å is also a semiconductor with a gap of 1.04 eV, as shown in Fig. 1(c). Like the armchair ribbons, when the width increases to 11.2 Å, the ZNR-as becomes metallic. For the ZNR-s, energy band calculations show that no matter how narrow the ribbons are, they are always metallic. The feature of energy band dispersions is not sensitive to the ribbon width as shown in Fig. 1(d). Thus, we conclude that ANR-as, ANR-s, and ZNR-as present a semiconductor–metal transition when the width of nanoribbon is increased. The origin of the width dependence for band-structures in B_2H_2 nanoribbons is attributed to the quantum-confinement effect.[28]

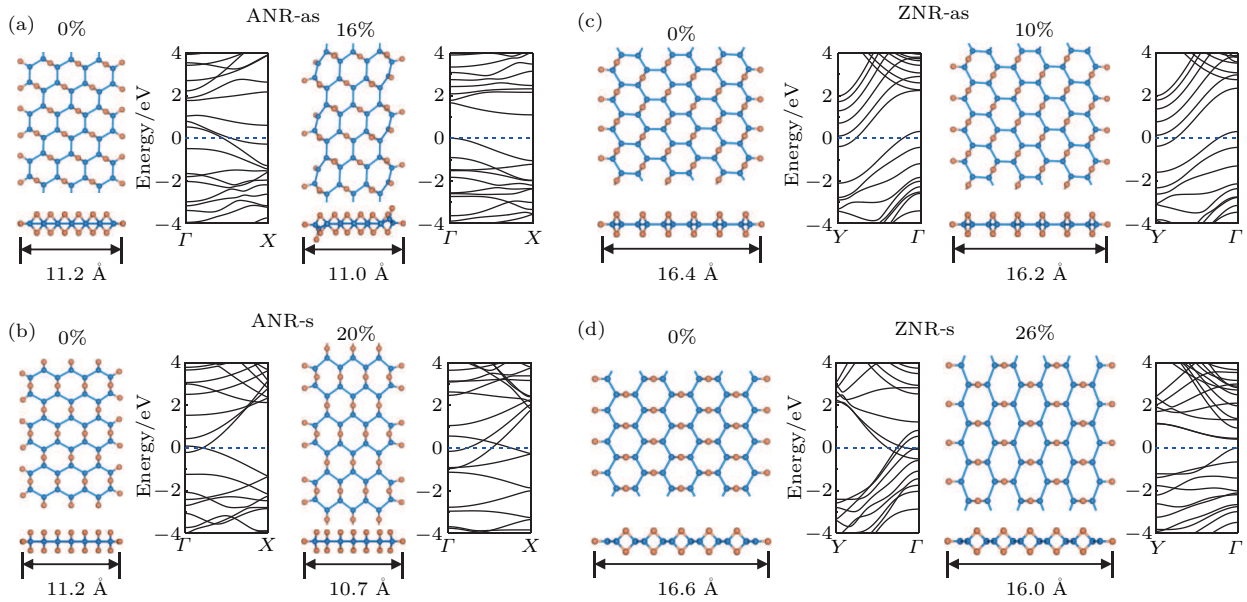

Fig. 2. Atomic structures and band structures of strained B_2H_2 nanoribbons. Atomic structures and corresponding band structures without and with strain are presented. Panel (a) is for ANR-as without and with 16% tensile strain. Panel (b) is for ANR-s without and with 20% tensile strain. Panel (c) is for ZNR-as without and with 10% tensile strain. Panel (d) is for ZNR-s without and with 26% tensile strain. The strain is labeled above each diagram.

As shown above, all four types of B_2H_2 ribbons are metallic when they are wider than 8.1 Å. We then investigate the possibility to switch the wide ribbons to semiconductors by applying tensile strain which is plausible due to the flexibility of B_2H_2. The experimentally applied strain on the 2D sample which is synthesized on substrate is usually less than 7% because of the limited elastic property of substrate. While for suspended 2D materials, the limited strain can be broken through by mechanical nano-indentation using atomic force microscope (AFM).[29]

We start from the armchair nanoribbon without mirror symmetry. Taking the ANR-as with a width of 11.2 Å as the example, when the strain increases, the ribbon becomes narrow. When the tensile strain is 16%, the width of ANR-as is reduced to 11.0 Å, as shown in Fig. 2(a). The saturated hydrogen atoms at the edge of ribbon are slightly displaced, but a complete honeycomb skeleton is still maintained. The corresponding electronic properties are shown in the right panel of Fig. 2(a). The strain-free ANR-as with a width of 11.2 Å is metallic. As the strain increases to 7%, the valence band maximum (VBM) approaches to the Fermi energy at Γ point, while the conduction band minimum (CBM) is near the Fermi level at X point. When the strain increases to 16%, the CBM departs away from the Fermi level, resulting in a gap of 1.10 eV.

We also investigate the strain effect of other ANR-as with different widths. As a 6.1-Å wide ANR-as, the strain-free ribbon is also metallic. When the strain increases to 8%, the VBM and CBM touch the Fermi level at Γ and X points, respectively. The ribbon begins to open a band gap if the strain continues to increase. When the strain is 18%, the gap reaches 1.39 eV. By studying the strain effect of different ribbon widths, we have found that a band gap can be opened under a certain tensile strain along the armchair direction.

The stability of nanoribbon under such a large tensile strain is then investigated by checking the existence of imaginary frequency, which is widely used in low-dimensional

materials.[30,31] Figure 3(a) is the phonon dispersion of a 11.0-Å ANR-as under 16% strain. There is no imaginary frequency, indicating that the strained ANR-as is structurally stable. Moreover, the electron localization function (ELF) of B–B bonds is analyzed and shown in Fig. 3(b). A large ELF value denotes that electrons are greatly localized between two atoms, which indicates that there are covalent bonds between atoms.

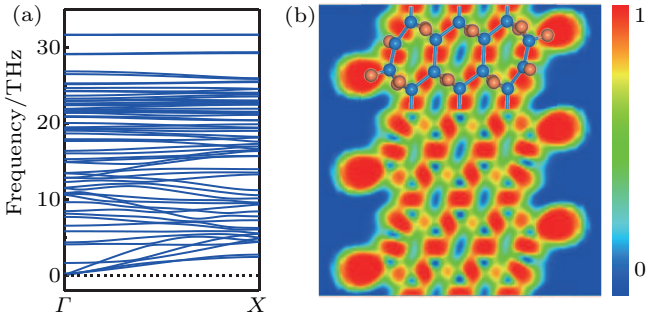

Fig. 3. The phonon dispersion and electron localization function of a B_2H_2 ANR-as under a 16% tensile strain. Panel (a) is the phonon dispersion. There is no imaginary frequency, indicating a stable structure. Panel (b) is the corresponding electron localization function. A large number (red) between two boron atoms indicates covalent bonds between atoms.

For a ZNR-s, a tensile strain along the zigzag direction can also open an energy gap. The band evolution of a wide ZNR-s has a similar trend to an ANR-as, as shown in Fig. 2(d). We find that even a 26% tensile strain is applied, the atomic structure remains similar, though the ribbon width has a shrink from 16.6 Å to 16.0 Å. The electronic properties are presented in the right panel accordingly. VBM and CBM touch at Fermi level under the 14% strain. A band gap of 0.37 eV is opened under a 26% strain, indicating the implementation of metal-semiconductor transition.

Applying a tensile strain along the armchair/zigzag direction cannot always open a band gap. For a wide ANR-s, the overlap of VBM and CBM, on the contrary, becomes larger under strain, as shown in Fig. 2(b). For the ZNR-as, the band structure is not sensitive to strain when the strain is smaller than 10%, as shown in Fig. 2(c). For the strain larger than 10%, the hexagonal boron skeleton is destroyed. Above all, a metal-semiconductor transition can be achieved by applying a tensile strain only for wide ANR-as and ZNR-s.

To further investigate why strain can open a gap in certain directions and cannot open gap in other directions, we study the strain effect on their 2D counterpart, B_2H_2 monolayer. Similar to the way to form B_2H_2 ribbons from cutting B_2H_2 monolayer, there are four crystalline directions in B_2H_2 monolayer (labeled in Fig. 4(a)). It has already been reported that applying a 20% tensile strain to B_2H_2 monolayer along the zigzag directions with mirror symmetry can open a gap of 0.38 eV.[19] They also found that when the strain is applied along the armchair direction with mirror symmetry, the sheet retains its metallic character. However, applying strain along the armchair and zigzag direction without mirror symmetry to B_2H_2 monolayer has not been investigated yet.

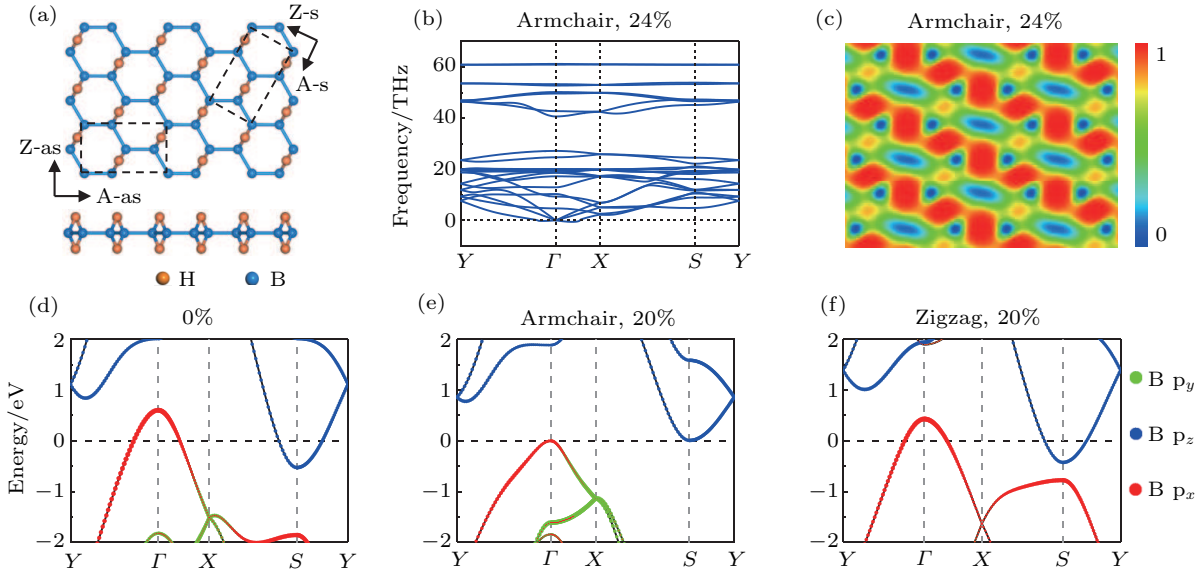

Fig. 4. The structural stability and band evolution of B_2H_2 monolayer. (a) The atomic structure of B_2H_2 monolayer. The four crystalline directions are labeled. (b) The phonon dispersion of a ZNR-as under 24% uniaxial strain. (c) The ELF of a ZNR-as under 24% uniaxial strain. Panels (d)–(f) are energy bands projected to boron atomic orbitals of B_2H_2 monolayer (d) without strain, (e) 20% tensile strain along armchair direction, and (f) 20% tensile strain along zigzag direction.

Therefore, we have investigated the electronic properties of B_2H_2 monolayer under strain along the armchair direction and zigzag direction. As a reference, we also present our calculated electronic structure of a strain-free B_2H_2 in Fig. 4(d), which is in agreement with previous work.[18,19] The CBM at Γ point is mainly contributed by the p_x orbital of boron atom, and the VBM at S point is mainly contributed by the p_z orbital of boron atom. While a strain is applied along the armchair direction, the CBM and VBM are gradually approaching the Fermi level. When the strain is 20%, as shown in

Fig. 4(e), they contact the Fermi level at Γ and S points, respectively. When the strain is 24%, a band gap of 0.12 eV is opened. In contrast, the metallic character is completely preserved for the strained sheet along the zigzag direction, as shown in Fig. 4(f). Through the strain effect analysis of B_2H_2 monolayer along four directions, we have found that in a B_2H_2 monolayer, applying a strain along an armchair direction without mirror symmetry or zigzag direction with mirror symmetry can open a gap. Therefore, the nanoribbons only by tailoring along such directions, that is ANR-as or ZNR-s, can open a band gap by applying strain. The band gap opening can be attributed to the breaking of the lattice symmetry of B_2H_2 sheet under strain.[32,33]

The B_2H_2 monolayer under such a large strain is also structurally stable. In the case of applying strain along the armchair direction, when the strain is 24%, there is no imaginary frequency in the phonon dispersion, as shown in Fig. 4(b). This implies that even under a 24% tensile strain along the armchair direction, the B_2H_2 monolayer remains stable. From the ELF calculation, we have also found a large value between neighbored boron atoms (as shown in Fig. 4(c)), which means the robustness of the B–B covalent bond. The band evolution for biaxial strain has a similar trend to the uniaxial strain along armchair direction. A gap of 0.11 eV is opened under 20% biaxial strain.

4. Conclusion

In summary, the electronic structures of B_2H_2 nanoribbons have been systematically investigated. It is firstly demonstrated that the electronic structure of B_2H_2 nanoribbons is sensitive to the ribbon width except for ZNR-s. Narrow ribbons generally present semiconducting feature. When ribbons are wider, a semiconductor–metal transition occurs, which is induced by the width. Then the possibilities of manipulation to the metallic feature of wide ribbons are further investigated by applying tensile strain. Two types of nanoribbons, ANR-as and ZNR-s, exhibit significant strain effect on band dispersion. When the strain exceeds a critical level, a band gap is opened. For example, a gap of 1.10 eV is opened under 16% strain for the 11.0-Å ANR-as. In contrast, applying a strain cannot open a gap in ANR-s and ZNR-as. Finally, the reason for the difference in strain effects in various ribbon types has also been investigated. We have found that such difference is mainly contributed by its unique atomic structure in 2D infinite sheet. Above all, the tunability of B_2H_2 nanoribbon electronic properties indicates that it is easier to find application space in nanoelectronic devices.

Acknowledgment

A portion of the research was performed in CAS Key Laboratory of Vacuum Physics. Computational resources were provided by the National Supercomputing Center in Tianjin.

References

[1] Mannix A J, Zhang Z, Guisinger N P, Yakobson B I and Hersam M C 2018 *Nat. Nanotechnol.* **13** 444
[2] Feng B, Sugino O, Liu R Y, Zhang J, Yukawa R, Kawamura M, Iimori T, Kim H, Hasegawa Y, Li H, Chen L, Wu K, Kumigashira H, Komori F, Chiang T C, Meng S and Matsuda I 2017 *Phys. Rev. Lett.* **118** 096401
[3] Zhang L Z, Yan Q B, Du S X, Su G and Gao H J 2012 *J. Phys. Chem. C* **116** 18202
[4] Zhang H, Li Y, Hou J, Du A and Chen Z 2016 *Nano Lett.* **16** 6124
[5] Liu X, Wei Z, Balla I, Mannix A J, Guisinger N P, Luijten E and Hersam M C 2017 *Sci. Adv.* **3** e1602356
[6] Guo W, Hu Y B, Zhang Y Y, Du S X and Gao H J 2009 *Chin. Phys. B* **18** 2502
[7] Penev E S, Bhowmick S, Sadrzadeh A and Yakobson B I 2012 *Nano Lett.* **12** 2441
[8] Wu X, Dai J, Zhao Y, Zhuo Z, Yang J and Zeng X C 2012 *ACS Nano* **6** 7443
[9] Liu Y, Penev E S and Yakobson B I 2013 *Angew. Chem. Int. Ed.* **52** 3156
[10] Li D, Chen Y, He J, Tang Q, Zhong C and Ding G 2018 *Chin. Phys. B* **27** 036303
[11] Mannix A J, Zhou X F , Kiraly B, Wood J D, Alducin D, Myers B D, Liu X, Fisher B L, Santiago U, Guest J R, Yacaman M J, Ponce A, Oganov A R, Hersam M C and Guisinger N P 2015 *Science* **350** 1513
[12] Feng B, Zhang J, Zhong Q, Li W, Li S, Li H, Cheng P, Meng S, Chen L and Wu K 2016 *Nat. Chem.* **8** 563
[13] Li W, Kong L, Chen C, Gou J, Sheng S, Zhang W, Li H, Chen L, Cheng P and Wu K 2018 *Chin. Sci. Bull.* **63** 282
[14] Xu L C , Du A and Kou L 2016 *Phys. Chem. Chem. Phys.* **18** 27284
[15] Abtew T A, Shih B-c, Dev P, Crespi V H and Zhang P 2011 *Phys. Lett. B* **83** 094108
[16] Abtew T A and Zhang P 2011 *Phys. Lett. B* **84** 094303
[17] Nishino H, Fujita T, Cuong N T, Tominaka S, Miyauchi M, Iimura S, Hirata A, Umezawa N, Okada S, Nishibori E, Fujino A, Fujimori T, Ito S I, Nakamura J, Hosono H and Kondo T 2017 *J. Am. Chem. Soc.* **139** 13761
[18] Jiao Y L, Ma F X, Bell J, Bilic A and Du A J 2016 *Angew. Chem. Int. Ed.* **55** 10292
[19] Mortazavi B, Makaremi M, Shahrokhi M, Raeisi M, Singh C V, Rabczuk T and Pereira L F C 2018 *Nanoscale* **10** 3759
[20] Zhang Y F, Zhang Y, Li G, Lu J, Que Y, Chen H, Berger R, Feng X, Müllen K, Lin X, Zhang Y Y, Du S, Pantelides S T and Gao H J 2017 *Nano Res.* **10** 3377
[21] Llinas J P, Fairbrother A, Borin Barin G, Shi W, Lee K, Wu S, Yong Choi B, Braganza R, Lear J, Kau N, Choi W, Chen C, Pedramrazi Z, Dumslaff T, Narita A, Feng X, Mullen K, Fischer F, Zettl A, Ruffieux P, Yablonovitch E, Crommie M, Fasel R and Bokor J 2017 *Nat. Commun.* **8** 633
[22] Pan J, Du S, Zhang Y, Pan L, Zhang Y, Gao H J and Pantelides S T 2015 *Phys. Lett. B* **92** 205429
[23] Pan L D, Zhang L Z, Song B Q, Du S X and Gao H J 2011 *Appl. Phy. Lett.* **98** 173102
[24] Kresse G and Furthmuller J 1996 *Phys. Lett. B* **54** 11169
[25] Blöchl P E 1994 *Phys. Lett. B* **50** 17953
[26] Perdew J P, Burke K and Ernzerhof M 1996 *Phys. Rev. Lett.* **77** 3865
[27] Baroni S, Gironcoli S d and Corso A D 2001 *Rev. Mod. Phys.* **73** 515
[28] Huang L F, Zhang G R, Zheng X H, Gong P L, Cao T F and Zeng Z 2013 *J. Phys.: Condens. Matter.* **25** 055304
[29] Lee C, Wei X, Kysar J W and Hone J 2008 *Science* **321** 385
[30] Zhang Y Y, Mishra R, Pennycook T J, Borisevich A Y, Pennycook S J and Pantelides S T 2015 *Adv. Mater. Interfaces* **2** 1500344
[31] Yin K, Zhang Y Y, Zhou Y, Sun L, Chisholm M F, Pantelides S T and Zhou W 2016 *2D Mater.* **4** 011001
[32] Zhou S Y, Gweon G H, Fedorov A V, First P N, de Heer W A, Lee D H, Guinea F, Castro Neto A H and Lanzara A 2007 *Nat. Mater.* **6** 770
[33] Ribeiro R M, Peres N M R, Coutinho J and Briddon P R 2008 *Phys. Lett. B* **78** 075442